



Scanning Magnetometry of Low Dimensional Electronic Systems

**Andrea Young
UNIVERSITY OF CALIFORNIA SANTA BARBARA**

**07/29/2019
Final Report**

DISTRIBUTION A: Distribution approved for public release.

**Air Force Research Laboratory
AF Office Of Scientific Research (AFOSR)/ RTB1
Arlington, Virginia 22203
Air Force Materiel Command**

REPORT DOCUMENTATION PAGE

*Form Approved
OMB No. 0704-0188*

The public reporting burden for this collection of information is estimated to average 1 hour per response, including the time for reviewing instructions, searching existing data sources, gathering and maintaining the data needed, and completing and reviewing the collection of information. Send comments regarding this burden estimate or any other aspect of this collection of information, including suggestions for reducing the burden, to Department of Defense, Washington Headquarters Services, Directorate for Information Operations and Reports (0704-0188), 1215 Jefferson Davis Highway, Suite 1204, Arlington, VA 22202-4302. Respondents should be aware that notwithstanding any other provision of law, no person shall be subject to any penalty for failing to comply with a collection of information if it does not display a currently valid OMB control number.
PLEASE DO NOT RETURN YOUR FORM TO THE ABOVE ADDRESS.

1. REPORT DATE (DD-MM-YYYY) 28-06-2019		2. REPORT TYPE Final		3. DATES COVERED (From - To) May 2016 - April 2019	
4. TITLE AND SUBTITLE Scanning Magnetometry of Low Dimensional Electronic Systems				5a. CONTRACT NUMBER	
				5b. GRANT NUMBER FA9550-16-1-0252	
				5c. PROGRAM ELEMENT NUMBER	
6. AUTHOR(S) Andrea F. Young				5d. PROJECT NUMBER	
				5e. TASK NUMBER	
				5f. WORK UNIT NUMBER	
7. PERFORMING ORGANIZATION NAME(S) AND ADDRESS(ES) The Regents of the University of California, Santa Barbara 3227 Cheadle Hall Santa Barbara, CA 93106				8. PERFORMING ORGANIZATION REPORT NUMBER	
9. SPONSORING/MONITORING AGENCY NAME(S) AND ADDRESS(ES) AFOSR				10. SPONSOR/MONITOR'S ACRONYM(S)	
				11. SPONSOR/MONITOR'S REPORT NUMBER(S)	
12. DISTRIBUTION/AVAILABILITY STATEMENT Distribution A - Approved or Public release					
13. SUPPLEMENTARY NOTES					
14. ABSTRACT The project successfully built and qualified a scanning probe microscope for magnetic and thermal imaging that operates at temperatures between 1.6-7.2K and in magnetic fields up to several tesla. We have used this to image a variety of materials, most notably atomically thin insulating ferromagnets, with one paper in preparation. We have also, in the course of our studies of twisted graphene heterostructures, made a major discovery of a new form of orbital magnetism supporting quantized electrical transport at zero magnetic field. This latter has far reaching applications for resistance metrology as well as ultra-low power electrically switchable magnetic memory storage.					
15. SUBJECT TERMS quantum electronics, low-power memory, quantum information processing, low-dimensional systems.					
16. SECURITY CLASSIFICATION OF:			17. LIMITATION OF ABSTRACT	18. NUMBER OF PAGES	19a. NAME OF RESPONSIBLE PERSON
a. REPORT	b. ABSTRACT	c. THIS PAGE			19b. TELEPHONE NUMBER (Include area code)

Final report on AFOSR Grant FA9550-16-1-0252, “Scanning Magnetometry of Low Dimensional Electronic Systems”

PI: Andrea Young

Lead institution: University of California, Santa Barbara

Executive summary of results and products: The project successfully built and qualified a scanning nanoSQUID on tip microscope that operates between 1.6-7.2K, and in magnetic fields up to several tesla. We have used this to image a variety of materials, most notably atomically thin insulating ferromagnets, with one paper in preparation. We have also, in the course of our studies of twisted graphene heterostructures, made a major discovery of a new form of *orbital magnetism* supporting quantized electrical transport at zero magnetic field. This latter has far reaching applications for resistance metrology as well as ultra-low power electrically switchable memories. An invention disclosure has been filed for this discovery and a paper describing the results is under review at *Science*. We expect one patent and two papers in high profile journals from this three year YIP award.

Original rationale for proposed research: Rapidly advancing progress in materials synthesis and device fabrication challenge existing experimental measurement techniques, demanding ever greater versatility, throughput, and sensitivity. Techniques capable of measuring multiple physical quantities, in situ, on the nanoscale are of particular value. Under the YIP award, the PI proposed to design a cryogenic scanning probe microscope for topographic, thermal, and magnetic imaging, based on a scanning nanoscale Superconducting QUantum Interference Device (SQUID) fabricated on the tip of a pulled quartz pipette. The -SQUID-on-tip (nSOT) microscope was proposed to bring unique capabilities to bear on topological states of matter, magnetic systems, and electronic devices by combining sub-single spin sensitivity, sub-mK thermal sensitivity, and <50 nm nanometer spatial resolution in a cryogenic, variable magnetic field environment. nSOT microscopy already far outstrips conventional scanning magnetometers along most metrics, and no other microscopy technique offers ultra-sensitive magnetometry and thermometry in a comparable regime of temperatures and magnetic fields. The proposed instrument was promised to enhance capabilities through the integration of topographic feedback, provide higher spatial resolution imaging and higher sensitivity to sample temperature, current, and magnetization. Our stated goals were to use the microscope to probe topological edge currents in 2D layered materials, perform precision thermal measurements of neutral mode transport in magnetic systems, and correlate magnetic structure and transport in low dimensional magnetic electron systems.

NanoSQUID on tip microscopy: Direct current SQUIDs have a long history as ultra-sensitive magnetometers. In a DC SQUID, two Josephson junctions embedded in a superconducting loop are measured in parallel. In the absence of a magnetic field (and for symmetric junctions), this causes the input current to bifurcate evenly along the two superconducting branches, with $I_{\{a,b\}} = I/2$ in the two branches, respectively. In the presence of a magnetic field, screening current (I_s) flows in the superconductor to cancel the external flux, leading to a current imbalance which drives one of the branches into a finite-voltage state when $I/2 + I_s > I_c$, the junction critical current. The energetics of flux screening in superconductors are periodic. Thus for applied flux $\Phi > \Phi_0/2$, the direction of the screening current reverses, with the balanced state ($I_a = I_b$) restored for $\Phi = \Phi_0$.

An ideal SQUID displays periodic oscillations of the critical current with periodicity Φ_0 , allowing sensitive readout of the external magnetic field.

Owing to the planar geometry of the superconducting circuit, which cannot easily be brought into close proximity with a planar sample, conventional scanning SQUID magnetometers are limited by low spatial resolution ($> 1 \mu\text{m}$). Moreover, in real DC SQUIDs the critical current does not oscillate indefinitely as a function of B , being limited by the formation of vortices in the SQUID or pickup loop. This limits the functional magnetic field range of conventional scanning SQUID magnetometers to a few mTesla.

nSOTs circumvent both the spatial resolution and B -field limits of conventional SQUIDs. nSOTs are fabricated on the apex of a pulled quartz pipette using a lithography-free self-aligned Pb-film deposition process in a home-built evaporator which allows liquid Helium cooling during the deposition to suppress Pb mobility (Fig. 1). The deposition produces Pb electrodes on two sides of the pipette connected by an apical ring that forms narrow Pb bridges between the macroscopic electrodes. Due to their sub-coherence length dimensions, the bridges form weak-link Josephson junctions, so that the tip forms a SQUID whose diameter can be varied between 30-250 nm. Because all dimensions of the superconductor, such as loop diameter and film thickness, are considerably smaller than the penetration depth, nSOTs maintain sensitivity up to magnetic fields of 1 T or more as no vortices can form in near the weak links.

Figure 2 shows characterization data from an 85 nm nSOT fabricated and measured at UCSB. Finite sensitivity was found up to at least 1T. Moreover, nSOTs typically include significant junction asymmetry, which leads to a near-absence of magnetic field 'blind spots'—in other words, for any B up to the maximum operating field of the nSOT, it is nearly always possible to choose a voltage bias such that the effective flux noise is on the order of $\approx 1 \mu\Phi_0/\sqrt{\text{Hz}}$, where $\Phi_0=h/2e$ is the superconducting flux quantum. Remarkably, flux noise is not degraded in smaller nSOTs, with the smallest nSOT fabricated at UCSB having a diameter of only 40 nm and showing similar characteristics.

At UCSB, we have constructed a scanning probe microscope based on nSOT tips. The microscope insert is housed in a large-capacity liquid Helium Dewar fitted with a 5 T solenoid magnet. The microscope insert is based on a pumped 4He pot/double-vacuum can design that allows operation in variable temperature between 1.5 and 7 K in high vacuum or variable pressure exchange gas. The dewar is supported on a 2-ton Pb-filled table supported on air springs, decreasing the relative motion between tip and sample due to vibrations to the sub-nm range.

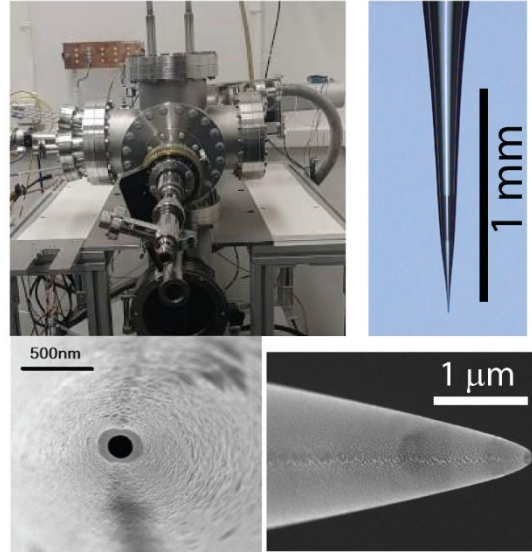


Figure 1: nSOTs are fabricated in a custom built thermal evaporator fitted with a Helium cryostat on a rotating flange. Various views of an nSOT tip.

Resolution in scanning magnetometry is limited in equal measure by the proximity of the sensor to the target and the size of the sensor itself, so that achieving high spatial resolution requires placing the tip in close proximity to the sample of interest. Unlike planar SQUIDs and scanning Hall probes, nSOTs permit arbitrarily proximate placement, as the sensor itself comprises the extremal part of the scanning probe. This geometry, however, comes with a drawback: unintentional contact with the sample can completely destroy the sensor, necessitating ex situ tip replacement. To address this issue, we have implemented topographic feedback using shear mode atomic force microscopy, in which the tip is mechanically coupled to a 32 kHz piezoelectric quartz tuning fork. Using an all electrical readout and actuation scheme we routinely achieve quality factors for the combined tuning fork-nSOT tip system between 25,000 and 50,000, which allows sensitive, all-electrical atomic force microscopy.

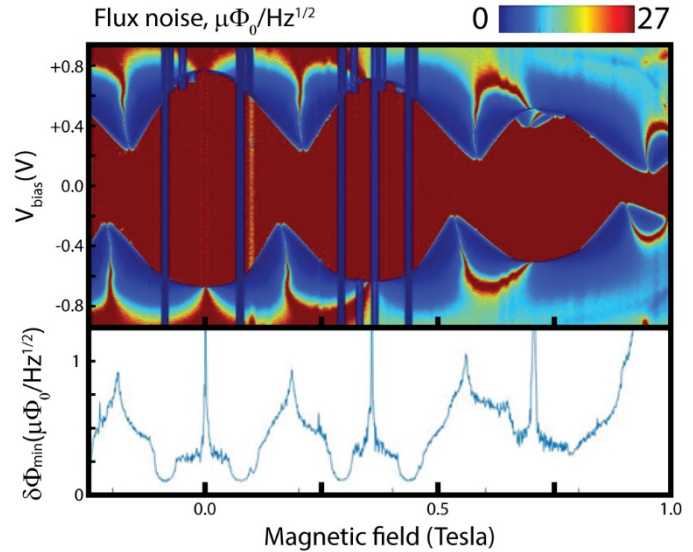


Figure 2: Noise characterization data for an 85 nm diameter nSOT. The upper panel shows the extracted magnetic field noise on a color scale as a function of nSOT bias applied V_{bias} and magnetic field B . On this plot, deep blue regions indicate regions of high sensitivity, while red regions indicate regions of low sensitivity. Vertical bands arise from feedback failure in the measurement circuit and not anomalous behavior of the nSOT. The lower panel shows the optimal sensitivity as a function of B : for nearly all B , a high flux sensitivity ($\delta\Phi < 1\mu\Phi_0/\sqrt{\text{Hz}}$) operating point can be found..

Conveniently, the same mechanical motion used in topographic feedback can be used for gradient magnetometry: for a translation of the nSOT tip \vec{r} at frequency f , a magnetometry signal will appear on the nSOT readout at frequency f proportional to $\partial B/\partial \vec{r}$. The in-plane direction of the oscillatory motion thus allows for measurements of, e.g., $\partial B_z/\partial x$, where B_z is the local static magnetic field. This signal appears at 32kHz, well above the $1/f$ knee in our nSOT system. Similar arguments obtain for measuring thermal gradients, for a 32kHz signal proportional to $\partial T/\partial x$. This

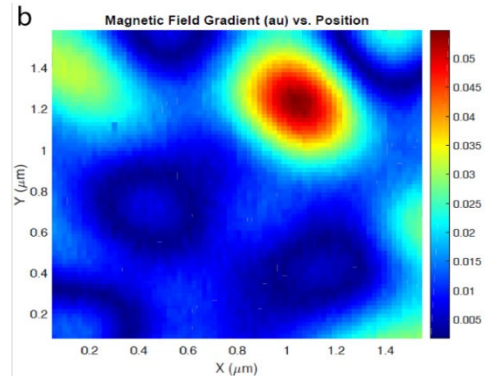


Figure 3: nSOT magnetic imaging of vortex state in a superconducting Pb film, taken by extracting the signal at the tuning fork resonance frequency.

allows static magnetic and thermal structure to be imaged without loss of sensitivity. An example of this imaging modality is shown in Figure 3, where the mixed vortex state of a Pb superconducting film is shown. In this measurement, the magnetic field *gradient* is plotted on the color scale, with high contrast features corresponding to large changes in the local B field, associated with clusters of pinned vortices.

Imaging of atomically thin layered ferromagnet CrI₃:

A subsequent target of our studies has been metal halides, in particular CrI₃, which is known to be an Ising ferromagnet at monolayer thickness but evolves to a layer antiferromagnet at multilayer thickness. In this case, the ground state at B=0 corresponds to fully polarized layers whose magnetization alternates. Magnetic fields of several hundred millitesla as sufficient to drive layer-by-layer transitions in the magnetization. Figure 4 shows magnetic images of a tetralayer CrI₃ flake. At low magnetic fields, the flake consists of two spin up and two spin down layers. At high magnetic fields, however, the magnetic ground state transitions, first to a 3up/1 down state and then to a 4 up/0 down state. The figure shows scanning magnetometry across the 2/2 to 3/1 transition. In the 2/2 state, the flake has no contrast, as the fringe fields of the antiferromagnet cancel to high precision on the 80nm scale of the nSOT probe. At high magnetic fields, in this case starting around 600 mT, contrast develops as a third layer polarizes.

We find that, unlike magnetically doped semiconductors, CrI₃ magnetizes via a discrete set of domain wall motions. This suggests that the magnetism is only very weakly pinned, save for at large-scale degradation sites, which are evident in our measurement as areas of enhanced contrast (rendered in red/yellow in Fig. 4). Ongoing efforts in this field involve trying to directly control interlayer interaction via interlayer twist.

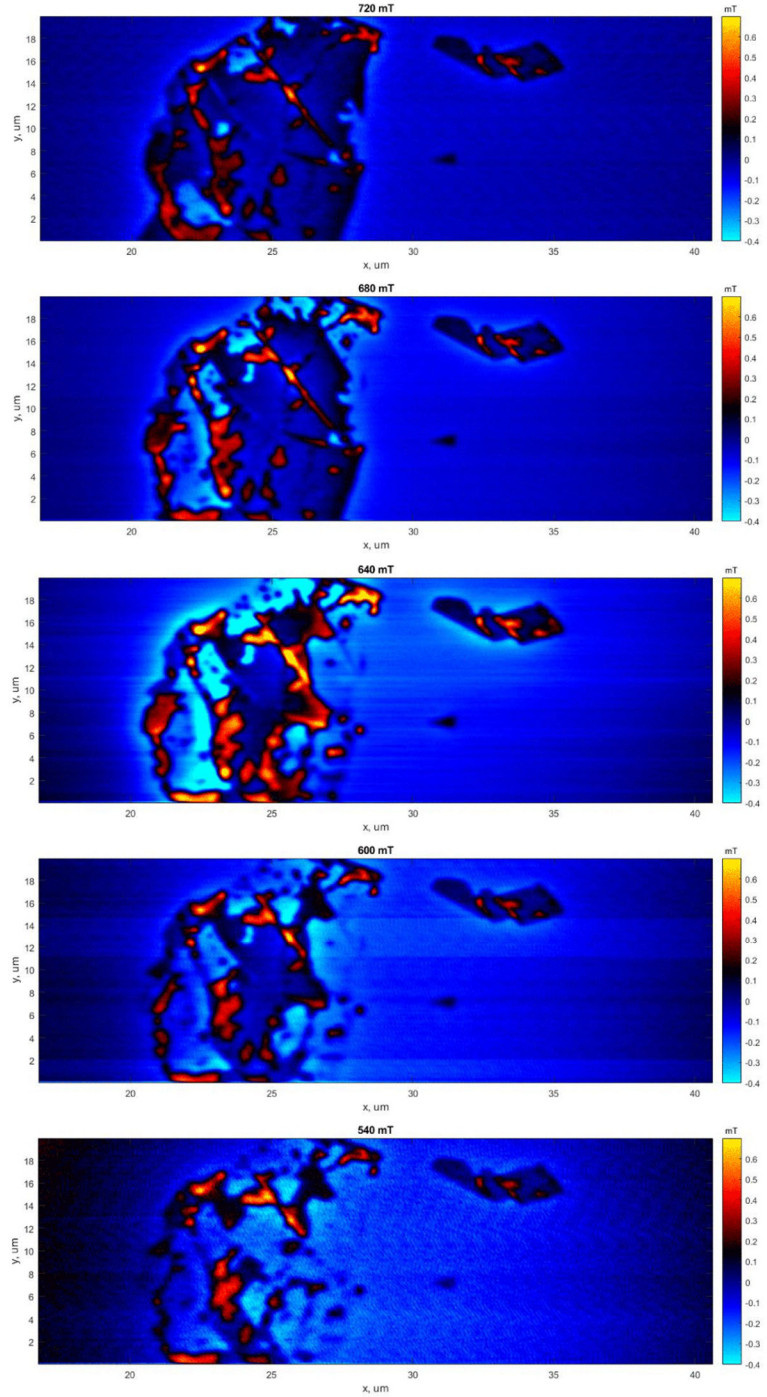


Figure 4: Magnetic imaging of tetralayer CrI₃. Successive images are taken at lower magnetic fields, and show the transition from a three-layer up/one layer down state to layer antiferromagnetic state (two up two down), which appears as a zero-contrast background. Bright red features are degradation due to reaction of CrI₃ flake ambient water prior to hBN encapsulation.

Intrinsic orbital magnetism and quantum anomalous Hall effect in twisted bilayer graphene:

Two dimensional insulators can be classified by the topology of their filled energy bands. In the absence of time reversal symmetry, nontrivial band topology manifests experimentally as a quantized Hall conductivity $\sigma_{xy} = C e^2/h$, where $C \neq 0$ is the total Chern number of the filled bands. Significant effort has been devoted to engineering quantum anomalous Hall (QAH) effects showing topologically protected quantized resistance in the absence of an applied magnetic field. To date, QAH effects have been observed only in a narrow class of materials consisting of transition metal doped $(Bi, Sb)_2 Te_3$. In these materials, ordering of the dopant magnetic moments breaks time reversal symmetry, combining with the strongly spin-orbit coupled electronic structure to produce topologically nontrivial Chern bands. However, the performance of these materials is limited by the inhomogeneous distribution of the magnetic dopants, which leads to microscopic structural, charge, and magnetic disorder. As a result, sub-kelvin temperatures are typically required to observe quantization, despite magnetic ordering temperatures at least one order of magnitude larger.

In our efforts to image magnetic states in van der Waals heterostructures under the YIP award, we discovered a new realization of this effect in an unexpected place—twisted bilayer graphene. Moiré graphene heterostructures provide the two essential ingredients---topological bands and strong correlations---necessary for engineering intrinsic quantum anomalous Hall effects. For both graphene on hexagonal boron nitride (hBN) and twisted multilayer graphene, moiré patterns generically produce bands with finite Chern number, with time reversal symmetry of the single particle band structure enforced by the cancellation of Chern numbers in opposite graphene valleys. In certain heterostructures, notably twisted bilayer graphene (tBLG) with interlayer twist angle $\theta \approx 1.1^\circ$ and rhombohedral graphene aligned to hBN, the bandwidth of these Chern bands

can be made exceptionally small, favoring correlation driven states that break one or more spin, valley, or lattice symmetries. Experiments have indeed found correlation driven low temperature phases at integer band fillings when these bands are sufficiently flat. Remarkably, states showing magnetic hysteresis indicative of time-reversal symmetry breaking have recently been reported in both tBLG and ABC/hBN heterostructures at commensurate filling. These systems show large anomalous Hall effects highly suggestive of an incipient Chern insulator at $B=0$.

While the experimental details of our work are found in our preprint, now under review, we summarize the main findings here. As shown in Figure 5, appropriately fabricated twisted bilayer graphene heterostructures can show a quantum anomalous Hall effect, with quantized Hall resistance of $\frac{h}{e^2} = 25.854 \text{ k}\Omega$. Remarkably, the effect is stable to several Kelvin—considerably higher than in other materials. QAH in twisted bilayer

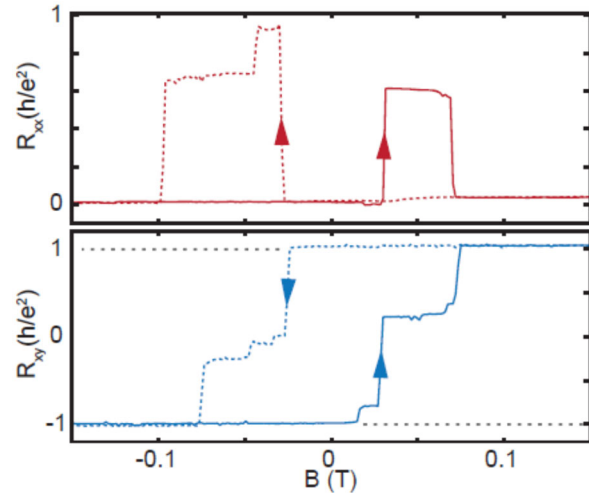


Figure 5: Quantized Hall resistance concomitant with vanishing longitudinal resistance measured as $B=0$ and 1.6K in twisted bilayer graphene.

graphene thus provides a possibly commercially compelling route to low-cost resistance metrology.

Perhaps even more compellingly, the intricate interplay between edge state transport and intrinsic magnetic order leads to a new route to electrically switchable magnetic memory. In our device, this allows deterministic electrical control over domain polarization using exceptionally small DC currents. Figure 6A shows R_{xy} at 6.5K and $B=0$, measured using a small AC excitation of ~ 100 pA to which we add a variable DC current bias. We find that the applied DC currents drive switching analogous to that observed in an applied magnetic field, producing hysteretic switching between magnetization states. DC currents of a few nanoamps are sufficient to completely reverse the magnetization, which is then indefinitely stable. Figure 6B shows deterministic writing of a magnetic bit using current pulses, and its nonvolatile readout using the large resulting change in the anomalous Hall resistance. High fidelity writing is accomplished with 20 nA current pulses while readout requires <100 pA of applied AC current.

Assuming a uniform current density in our micron-sized, two atom thick tBLG device results in an estimated current density $J < 10^4 A \cdot cm^{-2}$. While current-induced switching at smaller DC current densities has been realized in MnSi, readout of the magnetization state in this material has so far only been demonstrated using neutron scattering.

Compared with other systems that allow in situ electrical readout, such as GaMnAs and $Cr - (BiSb)_2Te_3$ heterostructures, the applied current densities are at least one order of magnitude lower. More relevant to device applications, the absolute magnitude of the current required to switch the magnetization state of the system ($\sim 10^{-9}A$ in our devices) is, to our knowledge, 3 orders of magnitude smaller than reported in any system.

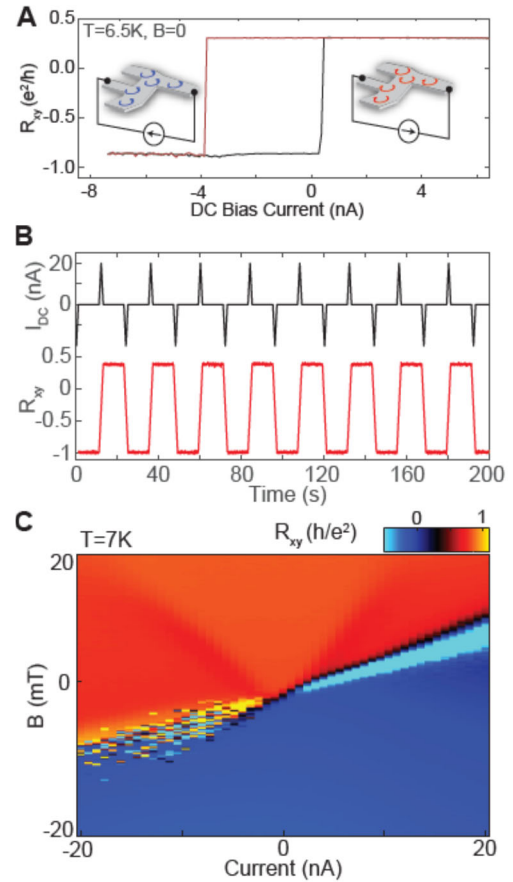


Figure 6: **A)** R_{xy} as a function of applied DC current, showing hysteresis as a function of DC current analogous to the response to an applied magnetic field. Insets: schematic illustrations of current controlled orbital magnetism. **B)** Nonvolatile electrical writing and reading of a magnetic bit at $T = 6.5K$ and $B=0$. A succession of 20 nA current pulses of alternating signs controllably reverses the magnetization, which is read out using the AC Hall voltage. The magnetization state of the bit is stable for at least 1000s. **C)** R_{xy} as a function of both DC bias current and magnetic field at 7K. Opposite directions of DC current preferentially stabilize opposite magnetization states of the bit.